Synthesis and Chemistry of $[Os_3(CO)_9(\mu_3\text{-}CCO)]^{2-}$. Metal Ensemble Effects on the Reactions of the CCO Ligand

Michael J. Went, Michael J. Sailor, Paula L. Bogdan, Carolyn P. Brock, and Duward F. Shriver*

Contribution from the Department of Chemistry, Northwestern University, Evanston, Illinois 60208. *Received February 24, 1987*

Abstract: The acylation of $[Os_3(CO)_{11}]^{2-}$ followed by reductive CO cleavage produces $[Os_3(CO)_9(CCO)]^{2-}$ (**1**) which undergoes a variety of reactions on the metal centers or the CCO ligand. Protonation yields $[HOs_3(CO)_9(CCO)]^-$ and the previously reported $H_2Os_3(CO)_9(CCO)$. The CCO ligand-centered reactions of **1** are dependent on the presence or absence of CO in the reaction. Hence under a CO atmosphere **1** is attacked by 2 equiv of $CH_3OSO_2CF_3$ to give the acetylene cluster $Os_3(CO)_{10}(CH_3C{\equiv}COCH_3)$ (**4**) while in the absence of CO the alkylidyne cluster $Os_3(CO)_9(\mu_3\text{-}CCH_3)(\mu_3\text{-}COCH_3)$ (**3**), along with a small amount of **4**, is produced. The origins of the reactivity differences between the $[M_3(CO)_9(CCO)]^{2-}$ clusters (M = Fe, Ru, Os) were explored from the standpoint of electronic structure and steric accessibility. A single-crystal X-ray structure determination of **1** reveals that the CCO ligand is tilted 26° away from the normal to the Os_3 plane toward one of the Os atoms. Thus it is structurally similar to $[Fe_3(CO)_9(CCO)]^{2-}$ but quite different from $[Ru_3(CO)_9(CCO)]^{2-}$. $[PPh_4]_2[Os_3(CO)_9(CCO)]$ crystallizes in the triclinic space group, $P\bar{1}$, with a = 12.762 (2) Å, b = 20.447 (5) Å, c = 10.779 (2) Å, α = 97.68 (2)°, β = 110.33 (2)°, and γ = 89.27 (2)°.

The dianionic iron ketenylidene $[Fe_3(CO)_9(CCO)]^{2-}$ has been shown to react with acid to cleave the C–C bond of the CCO ligand:[1]

$$[Fe_3(CO)_9(CCO)]^{2-} + R^+ \rightarrow [Fe_3(CO)_{10}(CR)]^-$$
$$R = H$$

More bulky electrophiles attack $[Fe_3(CO)_9(CCO)]^{2-}$ at the oxygen atom of the CCO ligand:[2]

$$[Fe_3(CO)_9(CCO)]^{2-} + R^+ \rightarrow [Fe_3(CO)_9(CCOR)]^-$$
$$R = CH_2CH_3,\ C(O)CH_3$$

Whereas in the reaction with $CH_3OSO_2CF_3$, both of the above reactions occur to give a 2:1 mixture of $[Fe_3(CO)_{10}(CCH_3)]^-$ and $[Fe_3(CO)_9(CCOCH_3)]^-$.[2]

By contrast the isoelectronic ruthenium ketenylidene $[Ru_3(CO)_9(CCO)]^{2-}$ protonates on the metal framework, leaving the CCO ligand intact.[3]

$$[Ru_3(CO)_9(CCO)]^{2-} + H^+ \rightarrow [(\mu\text{-}H)Ru_3(CO)_9(CCO)]^-$$

Initial attack by CH_3I also appears to occur at the metals.[4]

In this paper we report the synthesis and chemistry of the osmium ketenylidene $[Os_3(CO)_9(CCO)]^{2-}$ (**1**), thus completing a systematic survey of the effect of the metal identity on CCO reactivity for the iron triad. One interesting new twist in the chemistry of $[Os_3(CO)_9(CCO)]^{2-}$ illustrates the influence of the presence or absence of CO in determining the fate of the CCO ligand.

Experimental Section

Materials and Methods. All manipulations were performed under an atmosphere of prepurified N_2 using standard Schlenk techniques.[5] THF and Et_2O were dried over sodium benzophenone ketyl, pentane and hexane were dried over sodium, and CH_2Cl_2 was dried over P_2O_5. CD_2Cl_2 (99.6 + atom % D, Aldrich) was vacuum distilled from P_2O_5 prior to use. IR spectra were recorded on either a Perkin-Elmer 399 or 283 spectrophotometer using 0.1-mm path length CaF_2 solution cells. ^1H NMR spectra were recorded on a JEOL FX-270 spectrometer operating at 269.65 MHz, and ^{13}C NMR spectra were recorded on a JEOL FX-270 spectrometer operating at 67.80 MHz or a Varian XL-400 spectrometer operating at 100.58 MHz. All chemical shifts are reported positive if downfield relative to Me_4Si, using residual solvent protons (^1H) or the solvent (^{13}C) as internal references. ^{13}C NMR were recorded with $Cr(acac)_3$ added as a relaxation agent. [PPN]Cl and $[PPh_4]Br$ (Alfa) were used without further purification and $MeOSO_2CF_3$ (Aldrich) was distilled before use. Acetyl chloride was purified by distillation from PCl_5 followed by vacuum distillation from quinoline. Elemental analyses were performed by Schwarzkopf Microanalytical Laboratories. EI mass spectra were recorded at 15 and 70 eV, and the isotope envelope structure was fit by the program MASPAN.

Synthesis of $[PPN]_2[Os_3(CO)_9(CCO)]$ (1). To a solution of $[PPN]_2[Os_3(CO)_{11}]$ (0.290 g, 0.148 mmol)[6] in CH_2Cl_2 (12 mL) was added $CH_3C(O)Cl$ (11 μL, 0.155 mmol). The solution rapidly changed color from orange to yellow, indicating the formation of $[PPN][Os_3(CO)_{10}(COC(O)CH_3)]$. The solvent was reduced in volume under vacuum to ca. 5 mL and diethyl ether (40 mL) added to precipitate [PPN]Cl. The resulting solution was filtered and the solvent removed under vacuum. The residue was dissolved in THF (10 mL), and a THF solution of Na/Ph_2CO was added dropwise until the solution was orange and the IR spectrum showed complete consumption of $[PPN][Os_3(CO)_{10}(COC(O)CH_3)]$. The solvent was then removed under vacuum and the residue dissolved in CH_2Cl_2 (15 mL) containing [PPN]Cl (0.095 g, 0.166 mmol) and stirred for 20 min. The solution was then filtered through a Celite pad and $[PPN]_2[Os_3(CO)_9(CCO)]$ (**1**) (0.135 g, 47%) isolated as orange crystals by addition of diethyl ether (40 mL). An analogous procedure can be used to isolate **1** as a Ph_4P^+ salt. $[Os_3(*CO)_9(*C*CO)]^{2-}$ which is ^{13}C-enriched at all carbon atoms could be prepared by starting with ^{13}CO-enriched $[Os_3(*CO)_{11}]^{2-}$. Anal. Calcd for $C_{59}H_{40}O_{10}Os_3P_2$: C, 46.0; H, 2.6; Os, 37.0; P, 4.0. Found: C, 45.9; H, 2.7; Os, 37.1; P, 4.0. IR (CH_2Cl_2): ν_{CO} 2031 (w), 1994 (m), 1956 (vs), 1889 (m) cm^{-1}. ^{13}C NMR (CD_2Cl_2/CH_2Cl_2, +30 °C): 186.0 (s, 9 CO, $^1J_{^{187}OsC}$ = 42 Hz), 168.3 (s, C_β, $^1J_{CC}$ = 81 Hz), 31.2 (s, C_α, $^1J_{CC}$ = 81 Hz) ppm.

Synthesis of $[PPN][(\mu\text{-}H)Os_3(CO)_9(CCO)]$ (7). To a solution of $[PPN]_2[Os_3(CO)_9(CCO)]$ (0.20 g, 0.10 mmol) in CH_2Cl_2 (5 mL) was added $HOSO_2CF_3$ (9 μL, 0.10 mmol) dropwise. After the solution was stirred for 5 min, diethyl ether (30 mL) was added and the solution filtered to remove $[PPN][SO_3CF_3]$. The solvent was then removed under vacuum and the residue dissolved in diethyl ether (10 mL). Pentane (30 mL) was added to afford $[PPN][HOs_3(CO)_9(CCO)]$ (**7**) (0.018 g, 13%) as a yellow powder. Anal. Calcd for $C_{47}H_{31}NO_{10}Os_3P_2$: C, 40.3; H, 2.2; N, 1.0. Found: C, 40.1; H, 2.3; N, 1.1. IR (CH_2Cl_2): ν_{CO} 2075 (vw), 2035 (vs), 1997 (s), 1965 (m), 1912 (w) cm^{-1}. ^1H NMR (CD_2Cl_2, +20 °C): −20.01 ppm (s, 1 H, μ-H). ^{13}C NMR (CD_2Cl_2/CH_2Cl_2, +30 °C): 178.0 (s, 9 CO), 163.4 (s, C_β, $^1J_{CC}$ = 86 Hz), 17.2 ppm (s, C_α, $^1J_{CC}$ = 86 Hz). ^{13}C NMR (CD_2Cl_2/CH_2Cl_2, −90 °C): 185.6 (s, 1 CO) 183.3 (s, 2 CO), 179.9 (s, 2 CO), 172.9 (s, 2 CO) 168.2 (s, 2 CO), 162.5 (s, C_β, $^1J_{CC}$ = 86 Hz), 18.2 (s, C_α, $^1J_{CC}$ = 86 Hz) ppm.

Synthesis of $[PPN][Os_3(CO)_{10}(\mu_3\text{-}CCH_3)]$ (2). To a solution of $[PPN]_2[Os_3(CO)_9(CCO)]$ (0.20 g, 0.10 mmol) in CH_2Cl_2 (30 mL) was

(1) Kolis, J. W.; Holt, E. M.; Shriver, D. F. *J. Am. Chem. Soc.* **1983**, *105*, 7307.
(2) Hriljac, J. A.; Shriver, D. F. *J. Am. Chem. Soc.*, first of three papers in this issue.
(3) Sailor, M. J.; Shriver, D. F. *Organometallics* **1985**, *4*, 1476.
(4) Sailor, M. J.; Brock, C. P.; Shriver, D. F. *J. Am. Chem. Soc.*, second of three papers in this issue.
(5) Shriver, D. F.; Drezdzon, M. A. *Manipulation of Air-Sensitive Compounds*; 2nd ed.; Wiley: New York, 1986.
(6) Nagel, C. C.; Bricker, J. C.; Alway, D. G.; Shore, S. G. *J. Organomet. Chem.* **1981**, *219*, C9.

0002-7863/87/1509-6023$01.50/0

Table I. ^{13}C NMR Resonances and Carbon–Carbon Coupling Constants Associated with the CCO Ligand in Trimetallic Ketenylidene Clusters

compd	conditns	δ CCO	δ CCO	$^1J_{CC}$, Hz	ref
$[Fe_3(CO)_9(CCO)]^{2-}$	CD_3CN, −40 °C	90.1	182.2	74	1
$[Fe_3(CO)_7(SO_2)_2(CCO)]^{2-}$	CD_2Cl_2 8 −90 °C	6.6	167.4	89	23
$[Fe_2Co(CO)_9(CCO)]^-$	CD_2Cl_2, −90 °C	82.8	172.5	79	13
$[Co_2Mn(CO)_9(CCO)]^-$	CD_2Cl_2 8 −90 °C	73.3	170.5		14
$[Ru_3(CO)_9(CCO)]^{2-}$	CD_2Cl_2, −90 °C	−28.3	159.1	96	4
$[HRu_3(CO)_9(CCO)]^-$	THF-d_8, −90 °C	50.1	165.1	78	4
$H_2Ru_3(CO)_9(CCO)$	CD_2Cl_2, −90 °C	38.7	158.8	78	4
$[Os_3(CO)_9(CCO)]^{2-}$	CD_2Cl_2, 30 °C	31.2	168.3	81	*a*
$[HOs_3(CO)_9(CCO)]^-$	CD_2Cl_2, 30 °C	17.2	163.4	86	*a*
$H_2Os_3(CO)_9(CCO)$	$CDCl_3$, 25 °C	8.6	160.3	86	15
$[Co_3(CO)_9(CCO)]^+$	CD_2Cl_2, −110 °C	108.4	168.2		19
$[(Ph_3P)Co_3(CO)_8(CCO)]^+$	CD_2Cl_2, −90 °C		169.1		19
$[(CpMoCo_2(CO)_8(CCO)]^+$	CD_2Cl_2, −90 °C		158.0		19

[a] This work.

added dropwise 0.08 M $MeOSO_2CF_3/CH_2Cl_2$ solution (1.3 mL, 0.10 mmol). The resulting solution was stirred for 12 h and then the solvent removed under vacuum. The residue was extracted with diethyl ether (2 x 10 mL), and a product, formulated as $[PPN][Os_3(\mu\text{-CMe})(CO)_{10}]$ (**2**), was isolated as an orange oil by addition of pentane (20 mL). IR (CH_2Cl_2): ν_{CO} 2024 (s), 1971 (s, br) cm^{-1}. ^1H NMR (CD_2Cl_2, +20 °C): 4.12 (s, CH_3) ppm. ^{13}C NMR (CD_2Cl_2/CH_2Cl_2, +32 °C): 184.7 (s, 10 CO's); 167.7 (s, CCH_3) ppm. ^{13}C NMR (CD_2Cl_2/CH_2Cl_2, −90 °C): 249.3 (s, μ-CO), 177.1 (s, 9 CO's); 164.8 (s, CCH_3) ppm.

Synthesis of $(\mu\text{-H})Os_3(CO)_{10}(\mu_3\text{-CMe})$ (3). $[PPN][Os_3(CO)_{10}(\mu_3\text{-CMe})]$ (**2**) (see above) was dissolved in diethyl ether (15 mL) to which one drop of HBF_4OEt_2 was then added. The solution changed color from orange to yellow and was filtered after the addition of pentane (20 mL) to remove $[PPN][BF_4]$. Removal of the solvent under vacuum afforded $(\mu\text{-H})Os_3(CO)_{10}(\mu_3\text{-CMe})$ (**3**) as a yellow powder. Further purification was achieved by chromatography on an alumina column (1 × 10 cm) eluting with a 2:1 hexane/CH_2Cl_2 mixture. Collection of the yellow band and removal of the solvent under vacuum afforded $(\mu\text{-H})Os_3(CO)_{10}(\mu\text{-CMe})$ (**3**) (0.015 g, 17%). Mass spectrum: m/z 884 (MASPAN analysis of the parent envelope = 6.0%). Anal. Calcd for $C_{12}H_4O_{10}Os_3$: C, 16.4; H, 0.5. Found: C, 17.6; H, 0.8. IR (pentane): ν_{CO} 2112 (w), 2085 (mw), 2068 (vs), 2032 (s), 2023 (vs), 2012 (s), 2000 (vs) cm^{-1}. ^1H NMR (CD_2Cl_2, +20 °C): 4.54 (s, 3 H, Me), −16.91 (s, 1 H, μ-H) ppm. ^{13}C NMR (CD_2Cl_2/CH_2Cl_2, +1 °C): 297.7 (s, *C*Me), 174.3 (s, 2 CO), 174.1 (s, 4 CO), 173.1 (d, 2 CO, J_{CH} = 8.5 Hz), 168.9 (s, 2 CO) ppm.

Synthesis of $Os_3(CO)_9(\mu_3\text{-CMe})(\mu_3\text{-COMe})$ (5). $[PPN][Os_3(CO)_{10}(\mu\text{-CMe})]$ (**2**) (see above) was dissolved in CH_2Cl_2 (10 mL), and a 0.08 M solution of $MeOSO_2CF_3$ in CH_2Cl_2 (0.8 mL) was added. The solution was stirred for $1^1/_4$ h, solvent was removed under vacuum, and the solid was extracted with hexane (2 × 10 mL). Chromatography of the extracts on an alumina column (1.5 × 15 cm, 100% hexane) separated the product as a yellow band. Removal of the solvent under vacuum afforded $Os_3(CO)_9(\mu\text{-CMe})(\mu\text{-COMe})$ (**5**) (0.025 g, 27%) as a yellow powder. Mass spectrum: m/z 898 (MASPAN analysis of the parent envelope = 8.5%). Anal. Calcd for $C_{13}H_6O_{10}Os_3$: C, 17.5; H, 0.7. Found: C, 19.1; H, 1.0. IR (pentane): ν_{CO} 2062 (vs), 2022 (s), 2008 (s), 1994 (s) cm^{-1}. ^1H NMR (CD_2Cl_2 +20 °C): 4.67 (s, 3 H, COMe), 4.36 (s, 3 H, CMe, $^2J_{CH}$ = 6Hz) ppm. ^{13}C NMR (CD_2Cl_2/CH_2Cl_2, +30 °C): 312.5 (s, *C*OMe), 252.5 (s, *C*Me), 174.3 ppm (s, 9 CO).

Synthesis of $Os_3(CO)_{10}(\mu_3,\eta^2\text{-MeC}{=}COMe)$ (4). An 85-mg sample (0.044 mmol) of $[PPN]_2[Os_3(CO)_9(CCO)]$ (**1**) was dissolved in 4 mL of CH_2Cl_2. The solution was placed under an atmosphere of CO, and 12 μL (0.11 mmol) of $CH_3SO_3CF_3$ was syringed in. The solution was stirred for 5 h after which all but 0.5 mL of solvent was removed by pumping. Addition of 12 mL of hexane to the orange solution produced a white precipitate. The mixture was filtered, and the yellow filtrate was pumped to dryness. The yellow solid was extracted into pentane and cooled in a hexane slush bath, producing 0.015 g (36%) of **4** as a yellow powder. IR (pentane): ν_{CO} 2087 (w), 2062 (vs), 2043 (s), 2017 (w sh), 2007 (vs), 2002 (s), 2001 (m), 1984 (s), 1972 (m), 1949 (vw) cm^{-1}; mass spectrum: m/z 922 (MASPAN analysis of the parent envelope = 12.9%). ^1H NMR (CD_2Cl_2, 20 °C): 4.36 (br, 3 H, $COCH_3$), 2.47 (3 H, CCH_3). ^1H NMR (CD_2Cl_2, −20 °C): 4.34 (3 H, $COCH_3$), 2.45 (3 H, CCH_3). ^{13}C NMR (CD_2Cl_2, +20 °C): 300.6 (μ-CO), 243.6 (*C*OMe), 182.48 179.3, 179.0, 177.9, 176.0, 174.7, 174.2, 174.0, 172.0 (terminal CO's), 153.8 (*C*Me) ppm.

Extended Hückel Calculations. The $Fe_3(CO)_9$ unit was modeled as an array of C_{3v} symmetry by using bond lengths averaged from the single-crystal X-ray structure $[Ph_4As]_2[Fe_3(CO)_9(CCO)]$.[1] In one set of calculations the CCO ligand was placed along the 3-fold axis of the $Fe_3(CO)_9$ moiety with the α-carbon atom 1.25 Å above the plane of the metal triangle and with carbon–carbon and carbon–oxygen distances of 1.28 and 1.18 Å, respectively. To model the tilt of the CCO ligand as observed in the solid state structure, the α-carbon was moved parallel to the metal plane along a line perpendicular to an iron–iron bond until 2.00 Å from one metal center and 1.91 Å from the other two metals. The CCO vector was then inclined at an angle of 55° with respect to the metal plane. Extended Hückel calculations also were performed on a model in which the CCO ligand, tilted as described above, was incrementally rotated about an axis perpendicular to the metal plane passing through the center of the equilateral triangle.

The carbonyl ligand geometry exhibited in the solid state by $[PPN]_2[Ru_3(CO)_6(\mu\text{-CO})_3(CCO)]$[3] was modeled as follows: Three bridging carbonyl ligands were placed in the plane of the iron triangle with iron–carbon distances of 2.053 Å and carbon–oxygen distances of 1.154 Å. the two terminal carbonyl ligands per iron were given the same bond lengths as in the previous case (Fe–C, 1.760 Å; C–O, 1.154 Å), but one was moved such that the C–O vector was inclined 32° above the metal plane while the other was inclined 55° below the plane in accord with the crystallographic data for $[Ru_3(CO)_9(CCO)]^{2-}$.[3] In addition to the calculations reported here a large number of calculations were performed to check the sensitivity of the extended Hückel calculated energies and orbital coefficients. These included the use of the nonidealized bond lengths and angles taken directly from the crystal structures of $[Fe_3(CO)_9(CCO)]^{2-}$, $[Ru_3(CO)_9(CCO)]^{2-}$, and $[Os_3(CO)_9(CCO)]^{2-}$.[1,3] The indication from these calculations was that the use of the model structures did not bias our conclusions. Calculations were performed with the extended Hückel program ICON 8[7a] using orbital exponents and H_{ii} values reported in the literature.[7b]

Table II. X-ray Data for $[PPh_4]_2[Os_3(CO)_9(CCO)]$ (**1**)

formula	$C_{59}H_{10}O_{10}Os_3P_2$
fw	1541.52
D_{calcd}, g cm^3	1.963
cryst	irregular orange chunk, approx. size 0.5 × 0.4 × 0.3 mm
temp., °C	−120
space group	$P\bar{1}$
Z	2
a, Å	12.762 (2)
b, Å	20.447 (5)
c, Å	10.779 (2)
a, deg	97.68 (2)
β, deg	110.33 (2)
γ, deg	89.17 (2)
radiatn	Mo Kα, graphite monochromator
slit	4 mm
takeoff angle, deg	3.1
scan	ω–2θ, $2° < 2\theta < 55°$
range	$\pm h,k,\pm l$, h_{max} = 16, k_{max} = 26, l_{max} = 14
absorpt coeff (μ), cm^{-1}	74.2
range of transmissn coeff	0.99–0.60
no. of reflctns	11 933 total, 9614 observed

(7) (a) Program No. 344, Quantum Chemistry Program Exchange, Chemistry Department, Indiana University, Bloomington, IN, 47405. (b) Albright, T. A.; Hofmann, P.; Hoffmann, R. *J. Am. Chem. Soc.* **1977**, *99*, 7546.

Scheme I

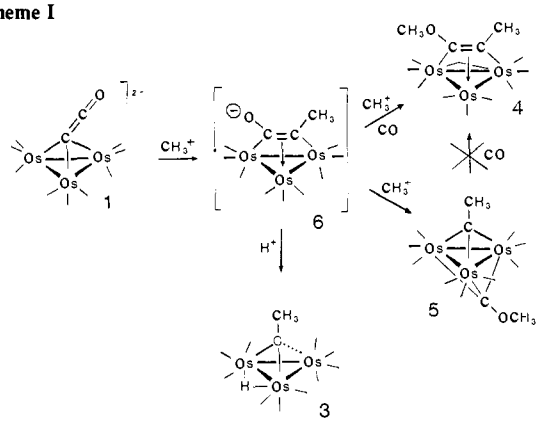

X-ray Structure Determination. Crystals were grown by diffusion of Et_2O into a CH_2Cl_2 solution of $[PPh_4]_2[Os_3(CO)_9(CCO)]$. A fragment of suitable size was cut from a larger chunk, mounted in air on a glass fiber and put into a nitrogen cold stream on an Enraf-Nonius CAD4 diffractometer. Relevant collection parameters are listed in Table II. The crystal system was found to be triclinic and the space group determined as $P\bar{1}$. The structure was solved with the Enraf-Nonius SDP Plus program package. The positions of the osmium atoms were determined by direct methods using program MULTAN. Most of the other atoms were located with another direct methods program, DIRDIF; the remainder found by subsequent difference fourier techniques. Scattering factors and corrections for anomalous dispersion were taken from the literature.[8] Hydrogen atoms were put in idealized positions and were used in the structure factor calculations but were not refined. All non-hydrogen atoms were refined anisotropically, and the refinement converged with a shift/error of 0.01 in the final cycle to $R = 2.7\%$ and $R_w = 3.5\%$. Correction for absorption was made with empirical psi scan data.

Results and Discussion

Alkylation Reactions. In its reactions the osmium ketenylidene cluster $[Os_3(CO)_9(CCO)]^{2-}$ (**1**) acts as a nucleophile. The reaction of **1** with 1 equiv of methyl trifluoromethanesulfonate followed by workup with acid produces the ethylidyne cluster **3** (eq 1).

$$\underset{\mathbf{1}}{[Os_3(CO)_9(CCO)]^{2-}} \xrightarrow{CH_3^+} \underset{\mathbf{2}}{[Os_3(CO)_{10}(CCH_3)]^-} \xrightarrow{H^+} \underset{\mathbf{3}}{HOs_3(CO)_{10}(CCH_3)} \quad (1)$$

The product **3** is the result of attack by the alkylating agent at the α-carbon of the CCO moiety with cleavage of the C_α–C_β bond. Similar C–C bond cleavage has been observed previously with the iron ketenylidene $[Fe_3(CO)_9(CCO)]^{2-}$.[1] The formulation of the alkylidyne **3** was confirmed by mass spectra, and its ^1H and ^{13}C NMR characteristics are in accord with those previously reported for the compounds $(\mu\text{-H})Os_3(CO)_{10}(\mu\text{-CR})$ (R = H, Ph, and CH_2CHMe_2).[9a-c]

Reaction of **1** with an excess of $CH_3OSO_2CF_3$ leads to incorporation of two methyl groups into the cluster, which produces two products dependent on the reaction conditions. As shown in Scheme I, the presence of carbon monoxide leads to the formation of the alkyne cluster $Os_3(CO)_{10}(MeC{\equiv}COMe)$ (**4**). Alternatively, if the reaction with excess $CH_3OSO_2CF_3$ is performed under N_2, scission of the CCO carbon-carbon bond occurs and the doubly capped alkylidyne cluster $Os_3(CO)_9(CMe)(COMe)$ (**5**) is formed along with a small amount of cluster **4**. The ready scission of the C–C bond of the CCO ligand is typical of the anionic iron triad ketenylidenes,[1,2,4] although in the context of osmium carbonyl cluster chemistry it is unusual. The osmium alkyne complex $Os_3(CO)_{10}(C_2Ph_2)$ will not undergo C–C cleavage even under forcing conditions but instead simply decarbonylates to the unsaturated species $Os_3(CO)_9(C_2Ph_2)$.[9d] By contrast, reversible alkyne C–C cleavage has been observed in the compound $Cp_2W_2Os(CO)_7(\mu_3\text{-}\eta^2\text{-}C_2Tol_2)$, albeit under the slightly forcing conditions of refluxing methylcyclohexane.[10] Both compounds **4** and **5** are formally electronically saturated clusters. The two capping alkylidyne ligands of **5** donate a total of six electrons to the cluster, resulting in an electron precise 48-electron cluster. The $(CCO)^{2-}$ ligand in the starting cluster **1** is also considered a 6-electron donor, so the transformation **1** → **5** involves no net change in the number of cluster valence electrons. The acetylene ligand in **4** is only a 4-electron donor, so the conversion of **1** to **4** requires the uptake of one CO to maintain a saturated 48-electron cluster.

The reversible coupling of alkylidyne ligands in the presence of CO to form a cluster-bound acetylene ligand has been observed with $Fe_3(CO)_9(\mu_3\text{-}CCH_3)(\mu_3\text{-}COC_2H_5)$ and with $Cp_2W_2Os(CO)_5(\mu\text{-}CTol)(\mu_3\text{-}CTol)$.[10,11] However, we are unable to observe the analogous conversion of **5** to **4**, even under forcing conditions (20 atm of CO, 24 h). This suggests that **5** is not an intermediate in the formation of **4** but that **5** and **4** are generated by separate pathways. The postulated intermediate **6** for formation of both **5** and **4** is shown in Scheme I. This compound is the result of attack of a methyl group on the α-carbon of the CCO without cleavage of the C_α–C_β bond. In the presence of CO, addition of a second methyl occurs on the oxygen of the CCO ligand, preserving the C_α–C_β bond and resulting in formation of the cluster-bound acetylene **4**. However, in the absence of CO, cleavage of the C_α–C_β bond occurs and the alkylidyne cluster **5** results. We interpret these results as follows. Addition of two alkyl groups oxidizes the ketenylidene cluster by two electrons. To compensate, the cluster can relieve its coordinate unsaturation by adding an extra CO ligand (formation of **4**), or if CO is unavailable, the extra two electrons needed are acquired through C–C bond cleavage of the ligand to yield the bicapped 48-electron cluster. The intermediate **6** is formulated as being analogous to the structurally characterized $[Fe_3(CO)_9(\mu_3,\eta^2\text{-}OC{=}CCH_3)]^{2-}$, which was generated by reductive coupling of an ethylidyne ligand with a carbonyl on $[Fe_3(CO)_9(\mu_3\text{-}CO)(\mu_3\text{-}CCH_3)]^-$.[12] Attempts to isolate the proposed intermediate **6** have been unsuccessful. A reddish orange oil can be obtained on workup after reaction of **1** with 1 equiv of $CH_3SO_3CF_3$. The product is formulated as $[PPN][Os_3(CO)_{10}(\mu_3\text{-}CCH_3)]$ (**2**) on the basis of spectroscopic evidence. In addition to the resonances of the $[PPN]^+$ counterion, the proton NMR of this oil has as its major resonance a singlet at 4.12 ppm. The infrared spectrum indicates that is a monoanion. The ^{13}C NMR spectrum at −90 °C contains three major resonances in addition to those of the CD_2Cl_2 solvent and the PPN^+ counterion, at 249.2, 177.1, and 164.8 ppm. The resonances at 249.2 and 177.1 appear to arise from one bridging and nine terminal carbonyl ligands, respectively, as both signals coalesce to a single resonance at 184.7 ppm at room temperature. Several smaller resonances appear in the terminal CO region of the spectrum and are attributed to impurities. The compound described above, **2**, can be converted to $HOs_3(CO)_{10}(\mu_3\text{-}CCH_3)$ (**3**) by protonation (eq 3) or to $Os_3(CO)_9(\mu_3\text{-}CCH_3)(\mu_3\text{-}COCH_3)$ (**5**) by further methylation (eq 4). Notably, methylation does not produce $Os_3(CO)_{10}(\mu_3,\eta^2\text{-}CH_3OC{=}CCH_3)$ (**4**), indicating that in the oil isolated after addition of 1 equiv of CH_3^+, CC bond scission of the former CCO ligand has already occurred (eq 2). Therefore the chemistry of the red-orange oil suggests it be formulated as $[Os_3(CO)_{10}(CCH_3)]^-$ (**2**). Although the ^{13}C NMR resonance assigned to the capping alkylidyne carbon, at 164.8 ppm, is much further upfield than previously reported capping alkylidyne resonances (these typically fall in the range 250 → 350 ppm),[9] the position of the resonance shows a temperature dependence characteristic of capping alkylidyne carbons. The resonance shifts to 167.7 ppm on raising the temperature from −90 to +32 °C.

(8) *International Tables for X-ray Crystallography*: The Kynoch Press: Birmingham, England, 1974; Vol. IV.

(9) (a) Shapley, J. R.; Cree-Uchiyama, M. E.; St. George, G. M.; Churchill, M. R.; Bueno, C. *J. Am. Chem. Soc.* **1983**, *105*, 140. (b) Yeh, W.-Y.; Shapley, J. R.; Li, Y.; Churchill, M. R. *Organometallics* **1985**, *4*, 767. (c) Green, M.; Orpen, A. G.; Schaverien, C. J. *J. Chem. Soc., Chem. Commun.* **1984**, 37. (d) Tachikawa, M.; Shapley, J. R.; Pierpont, C. G. *J. Am. Chem. Soc.* **1975**, *97*, 7172.

(10) Chi, Y.; Shapley, J. R. *Organometallics* **1985**, *4*, 1900.

(11) Nuel, D.; Dahan, F.; Mathieu, R. *Organometallics* **1985**, *4*, 1436.

(12) Dahan, F.; Mathieu, R. *J. Chem. Soc. Chem. Commun.* **1984**, 432.

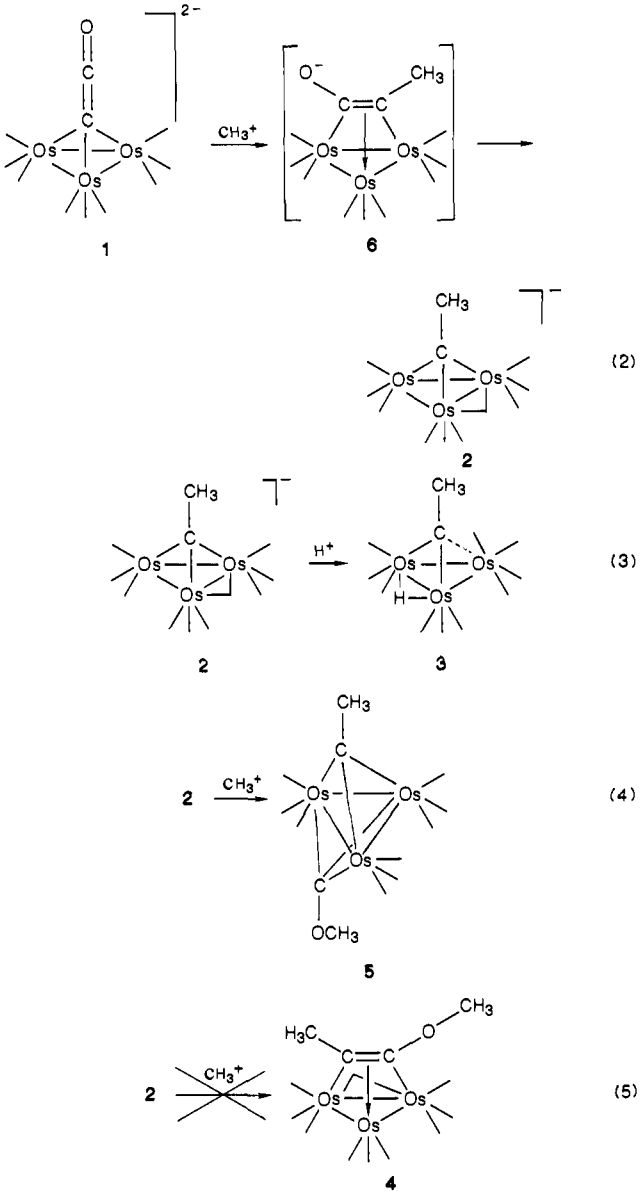

As observed for the triruthenium ketenylidene cluster $[Ru_3(CO)_9(CCO)]^{2-}$, the triosmium cluster **1** is protonated on the metal framework (Scheme II).[3] This is in contrast to the isostructural iron analogue, which is observed to undergo protonation on the α-carbon of the CCO ligand with concomitant cleavage of the C_α–C_β bond and subsequent migration of the ketenylidene CO down onto the metal framework.[1] The mixed-metal ketenylidenes $[Fe_2Co(CO)_9(CCO)]^-$ and $[Co_2Mn(CO)_9(CCO)]^-$ have also been observed to protonate on the α-carbon of the CCO with cleavage of the C–CO bond.[13,14] The observed attack of protons on the metal skeleton of the ruthenium and osmium clusters is consistent with the increased basicity of second- and third-row metals over those in the first row. The reaction of $[PPN]_2[Os_3(CO)_9(CCO)]$ with successive equivalents of HCl in a resealable NMR tube results first in formation of $[HOs_3(CO)_9(CCO)]^-$. Addition of more HCl leads to $H_2Os_3(CO)_9(CCO)$, and finally the cationic ketenylidene $[H_3Os_3(CO)_9(CCO)]^+$, as determined by ^1H NMR. The compounds $H_2Os_3(CO)_9(CCO)$ and $[H_3Os_3(CO)_9(CCO)]^+$ have been previously characterized.[15]

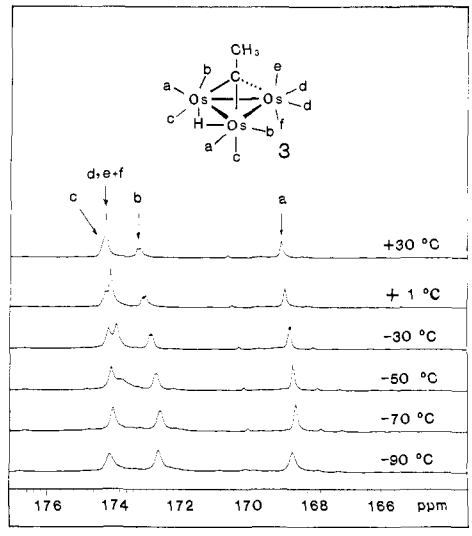

Figure 1. Variable-temperature ^{13}C NMR spectra and assignments for $HOs_3(CO)_{10}(\mu\text{-}CCH_3)$ (**3**) in the carbonyl region.

Scheme II

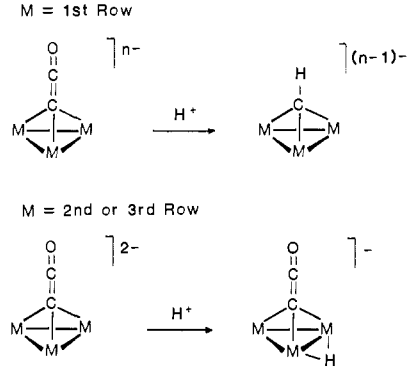

Spectroscopy. The formation of the ketenylidene $[Os_3(CO)_9(CCO)]^{2-}$ (**1**) was confirmed by the ^{13}C NMR spectrum of **1** produced from $Os_3(CO)_{12}$ which was ca. 40% enriched with ^{13}CO. The spectrum contains resonances assigned to the capping carbon (C_α) at 31.2 ppm and the ketenylidene carbonyl (C_β) at 168.3 ppm. Both resonances show satellites corresponding to carbon–carbon coupling of 81 Hz, which is similar in magnitude to that observed for other trimetallic ketenylidenes and reflects the high C–C bond order. The ^{13}C NMR resonances of the CCO ligand both appear upfield of the terminal carbonyl resonances, as has typically been observed in these compounds (see Table I). The β-carbon resonance is invariably found in the region from 155 to 185 ppm, and in **1** it is at 168.3 ppm. The α-carbon resonances in these clusters are observed over a larger chemical shift range although they are always upfield of the β-carbon resonances. These fall in the region from −30 to 110 ppm, and in **1** the α-carbon resonates at 31.2 ppm. The nine carbonyl ligands are equivalent on the NMR time scale at room temperature, as shown by the single resonance at 186.0 ppm. This signal has satellites of integrated intensity ca. 5% with respect to the central peak and are postulated to be due to coupling to the ^{187}Os nucleus which has a nuclear spin of $^1/_2$ and is 1.64% naturally abundant. The coupling constant $^1J_{^{187}Os-^{13}C}$ is 42 Hz and is comparable to the reported value of $J_{^{187}Os-^{13}C}$ in $^{187}Os_3(CO)_{12}$, 33 Hz.[16] Upon cooling to −90 °C the signal at 186.0 ppm broadens and collapses and two new signals at 190.9 and 181.1 ppm appear in the ratio 1:2 and remain down to −140 °C. This can be interpreted as either the freezing out of the $(CO)_3$ turnstile motion at the osmium centers or a freezing out of the CCO precession motion. The extended Hückel calculations discussed below suggest that the

(13) Kolis, J. W.; Holt, E. M.; Hriljac, J. A.; Shriver, D. F. *Organometallics* **1984**, *3*, 496.
(14) Crespi, A. M.; Shriver, D. F. *Organometallics* **1986**, *5*, 1750.
(15) (a) Sievert, A. C.; Strickland, D. S.; Shapley, J. R.; Steinmetz, G. R.; Geoffroy, G. L. *Organometallics* **1982**, *1*, 214. (b) Shapley, J. R.; Strickland, D. S.; St. George, G. M.; Churchill, M. R.; Bueno, C. *Organometallics* **1983**, *2*, 185.
(16) Koridze, A. A.; Kizas, O. A.; Astakhova, N. M.; Petrovski, P. V.; Grishin, Y. K. *J. Chem. Soc. Chem. Commun.* **1981**, 853.

potential energy surface for the precession of the CCO is very flat.

Reaction of $[PPN]_2[Os_3(CO)_9(CCO)]$ with 1 equiv of $HOSO_2CF_3$ leads to the formation of $[PPN][HOs_3(CO)_9(CCO)]$. The bridging hydride ligand is observed in the ^1H NMR spectrum at −20.01 ppm, and the ^{13}C NMR spectrum indicates that the CCO ligand remains intact. The α-carbon resonates at 17.2 ppm and the β-carbon at 163.4 ppm with $^1J_{CC}$ = 86 Hz. These resonances are intermediate in position between those observed for $[PPN]_2[Os_3(CO)_9(CCO)]$ and $H_2Os_3(CO)_9(CCO)$ (see Table I), indicating that protonation is not causing a large structural change. At room temperature, the nine CO ligands are equivalent at 178.0 ppm, but at −90 °C five CO resonances are observed in the ratio 1:2:2:2:2, indicating that the molecule contains a mirror plane consistent with the structure shown.

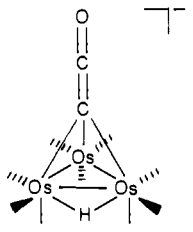

Reaction of $[PPN]_2[Os_3(CO)_9(CCO)]$ with 1 equiv of $MeOSO_2CF_3$ followed by protonation affords $(\mu\text{-H})Os_3(CO)_{10}(\mu_3\text{-CMe})$ (**3**). The formulation of $(\mu\text{-H})Os_3(CO)_{10}(\mu_3\text{-CMe})$ was confirmed by mass spectra and NMR spectroscopy. The ^{13}C NMR of **3** at 1 °C shows four carbonyl resonances at 174.3, 174.1, 173.1, and 168.9 ppm in the ratio 2:4:2:2, assigned to c, d + e + f, b, and a of Figure 1, respectively. The resonance at 173.1 ppm is a doublet under conditions of proton coupling ($^1J_{CH}$ = 8.5 Hz) and thus is attributed to trans coupling of the carbonyls b with the hydride. At −90 °C, the lowest temperature at which the ^{13}C NMR spectrum was recorded, the resonance due to the carbonyls d + e + f collapsed, but the low-temperature limit as observed for the Ph and H derivatives[9a,b] was not achieved. On cooling from +30 to −90 °C the resonance assigned to the alkylidene carbon shifts from 299.3 to 293.3 ppm. Such temperature dependence of the capping carbon resonance is a spectral characteristic which has been noted for other complexes of this type.[9a,b] The ^1H NMR reveals resonances due to the methyl group at 4.54 ppm and the bridging hydride at −16.91 ppm.

Reaction of **1** with 2 equiv of $MeOSO_2CF_3$ results in cleavage of the C–CO bond to form $Os_3(CO)_9(\mu\text{-CMe})(\mu\text{-COMe})$ (**5**) in an analogous manner to the methylation of $[Fe_3(CO)_{10}(\mu\text{-CMe})]^-$.[2] A similar triosmium complex with two capping alkylidyne ligands has been reported.[17] ^1H NMR shows signals due to the two methyl groups at 4.67 and 4.36 ppm assigned to COMe and CMe groups, respectively. Proton NMR spectra of $Os_3(CO)_9(\mu\text{-CMe})(\mu\text{-COMe})$ prepared from ^{13}C enriched $[PPN]_2[Os_3(CO)_9(CCO)]$ show ^{13}C satellites for the resonance at 4.36 ppm ($^2J_{CH}$ = 6 Hz). The ^{13}C NMR has resonances assigned to the two capping alkylidene carbons at 312.5 (COMe) and 252.5 (CMe) ppm and a signal due to the nine carbonyl ligands at 174.3 ppm. The carbonyl resonance remains a singlet down to −90 °C.

Alternatively, the alkyne complex $Os_3(CO)_{10}(MeC{\equiv}COMe)$ (**4**) is formed when $[PPN]_2[Os_3(CO)_9(CCO)]$ reacts with 2 equiv of $MeOSO_2CF_3$ under an atmosphere of CO. The complex $Os_3(CO)_{10}(MeC{\equiv}COMe)$ has a molecular ion envelope in the mass spectrum centered at m/z 922 confirming it to be the product of two methylations and carbon monoxide incorporation (MASPAN analysis of the isotopic envelope yields a fit of R = 12.9% for the formula of **4**). The presence of an alkyne ligand is confirmed by resonances at 243.6 and 153.8 ppm in the ^{13}C NMR spectrum. The corresponding resonances in the iron analogue $Fe_3(CO)_{10}(MeC{\equiv}COEt)$ occur at 224.8 and 155.6 ppm.[11] The ^1H NMR shows two methyl resonances at 4.36 (COMe) and 2.47 ppm (CMe). The COMe resonance is broad at room temperature and sharpens upon cooling to −20 °C, indicating that there is restricted rotation about the C–O bond. A resonance at 300.6 ppm in the ^{13}C NMR spectrum of **4** is assigned to a bridging carbonyl ligand. We were, however, unable to observe a bridging carbonyl absorbance in the solution infrared spectrum of **4**.

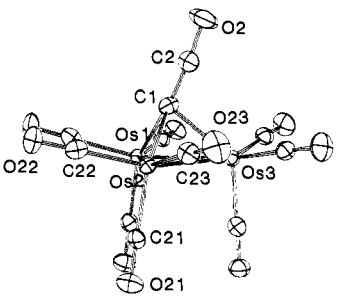

Figure 2. ORTEP diagram of the anionic portion of $[Ph_4P]_2[Os_3(CO)_9(CCO)]$ (**1**) showing the atom-numbering scheme. The CCO ligand is tilted toward Os(3) by 26° from the perpendicular to the metal triangle. Thermal ellipsoids are drawn at 50% probability level.

Table III. Bond Distances (Å) and Angles (deg) for **1**

atom 1	atom 2	dist	atom 1	atom 2	dist
Os1	Os2	2.7439 (2)	Os3	C31	1.885 (5)
Os1	Os3	2.7512 (2)	Os3	C32	1.889 (4)
Os2	Os3	2.7634 (2)	Os3	C33	1.899 (5)
Os1	C1	2.133 (4)	C11	O11	1.156 (6)
Os1	C11	1.892 (4)	C12	O12	1.149 (6)
Os1	C12	1.898 (5)	C13	O13	1.149 (6)
Os1	C13	1.899 (5)	C21	O21	1.158 (6)
Os2	C1	2.111 (5)	C22	O22	1.142 (6)
Os2	C21	1.889 (4)	C23	O23	1.147 (6)
Os2	C22	1.903 (5)	C31	O31	1.153 (6)
Os2	C23	1.903 (5)	C32	O32	1.156 (6)
Os3	C1	2.205 (4)	C33	O33	1.158 (7)
Os3	C2	2.814 (5)	C2	O2	1.187 (6)
			C1	C2	1.269 (7)

atom 1	atom 2	atom 3	angle	atom 1	atom 2	atom 3	angle
Os2	Os1	Os3	60.380 (5)	C21	Os2	C23	101.2 (2)
Os1	Os2	Os3	59.942 (5)	C22	Os2	C23	101.6 (2)
Os1	Os3	Os2	59.679 (5)	C31	Os3	C32	99.1 (2)
C11	Os1	C12	99.8 (2)	C31	Os3	C33	99.2 (2)
C11	Os1	C13	98.5 (2)	C32	Os3	C33	101.0 (2)
C12	Os1	C13	105.3 (2)	O2	C2	C1	175.5 (5)
C21	Os2	C22	93.9 (2)				

Structure of $[PPh_4]_2[Os_3(CO)_9(CCO)]$. The dianion $[Os_3(CO)_9(CCO)]^{2-}$ (**1**) is isostructural with $[Fe_3(CO)_9(CCO)]^{2-}$ but is significantly different from its protonated analogue $H_2Os_3(CO)_9(CCO)$. The compound $[Ph_4P]_2[Os_3(CO)_9(CCO)]$ crystallizes in the triclinic space group $P\bar{1}$ with two cation dianion combinations per unit cell. There are no close cation–anion contacts. The three osmium atoms form an approximate equilateral triangle [Os(1)–Os(2) = 2.744 (1), Os(1)–Os(3) = 2.751 (1), and Os(2)–Os(3) = 2.763 (1) Å]. The metal–metal bonds are shorter than those found in $Os_3(CO)_{12}$ (average Os–Os = 2.8771 (27) Å).[18] As shown in Figure 2, the carbonyl groups of **1** are disposed around the osmium triangle as a set of three axial and six equatorial ligands, the osmium–carbon distances being the same within error [average Os–C = 1.895 (2) Å]. The ketenylidene is coordinated by C(1) on top of the $Os_3(CO)_9$ base. The bond distances C(1)–C(2) = 1.269 (7) Å and C(2)–O(2) = 1.187 (6) Å are similar to the analogous distances in $[Fe_3(CO)_9(CCO)]^{2-}$ (1.28 (3) and 1.18 (3) Å),[1] $[Ru_3(CO)_9(CCO)]^{2-}$ (1.300 (10) and 1.171 (8) Å),[3] and $H_2Os_3(CO)_9(CCO)$ (1.264 (37) and 1.154 (34) Å).[15] The ketenylidene ligand is approximately linear (C(1)–C(2)–O(2) = 175.5 (5)°) and is tilted over an osmium center Os(3) by an angle of 26° between the least-squares line through C-

(17) Yeh, W.-Y.; Shapley, J. R.; Ziller, J. W.; Churchill, M. R. *Organometallics* **1986**, *5*, 1757.

(18) Churchill, M. R.; DeBoer, B. G. *Inorg. Chem.* **1977**, *16*, 878.

Table IV. Positional Parameters and Their Estimated Standard Deviations for **1**

atom	x	y	z	B, Å²
Os1	0.62974 (1)	0.31308 (1)	0.41419 (2)	1.499 (3)
Os2	0.55647 (1)	0.29305 (1)	0.14001 (2)	1.436 (3)
Os3	0.51038 (1)	0.19884 (1)	0.27720 (2)	1.428 (3)
O11	0.8650 (3)	0.2671 (2)	0.4474 (4)	2.76 (8)
O12	0.6144 (3)	0.2842 (2)	0.6776 (4)	2.53 (7)
O13	0.6750 (4)	0.4615 (2)	0.4462 (5)	3.39 (9)
O21	0.7808 (3)	0.2493 (2)	0.1230 (4)	2.99 (8)
O22	0.5847 (4)	0.4321 (2)	0.0818 (5)	3.41 (9)
O23	0.3923 (4)	0.2285 (3)	−0.1273 (4)	3.5 (1)
O31	0.7247 (3)	0.1259 (2)	0.3036 (4)	2.63 (8)
O32	0.3532 (4)	0.1095 (2)	0.0375 (4)	3.16 (9)
O33	0.4552 (4)	0.1486 (2)	0.5030 (4)	3.05 (8)
O2	0.2702 (4)	0.3089 (3)	0.2637 (6)	4.3 (1)
C1	0.4644 (4)	0.3031 (3)	0.2704 (5)	1.91 (9)
C2	0.3642 (4)	0.3038 (3)	0.2680 (5)	2.26 (9)
C11	0.7766 (4)	0.2848 (3)	0.4387 (5)	2.06 (9)
C12	0.6181 (4)	0.2964 (3)	0.5782 (5)	1.98 (9)
C13	0.6584 (4)	0.4056 (3)	0.4355 (5)	2.4 (1)
C21	0.6936 (4)	0.2656 (3)	0.1233 (4)	1.82 (8)
C22	0.5737 (4)	0.3803 (3)	0.1048 (5)	2.4 (1)
C23	0.4527 (4)	0.2538 (3)	−0.0269 (5)	2.22 (9)
C31	0.6429 (4)	0.1530 (3)	0.2941 (5)	1.99 (9)
C32	0.4109 (4)	0.1448 (3)	0.1277 (5)	2.02 (9)
C33	0.4756 (4)	0.1691 (3)	0.4184 (5)	2.12 (9)

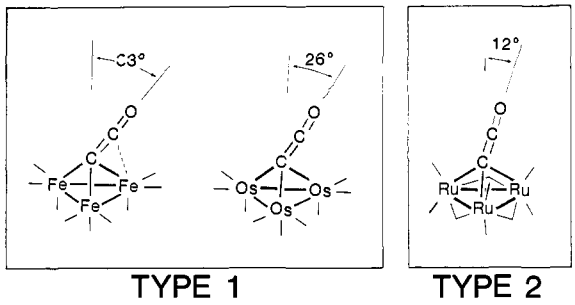

Figure 3. The carbonyl and CCO ligand orientations in the dianionic trimetallic clusters $[M_3(CO)_9(CCO)]^{2-}$ (M = Fe, Ru, Os). Clusters of type 1 are characterized by a set of three axial and six equatorial carbonyls and a pronounced tilt of the CCO ligand toward a metal vertex. Type 2 has two sets of three terminal carbonyls above and below the metal plane and a third set of three bridging carbonyls roughly in the plane of the trimetal framework. In type 2 the CCO is slightly tilted toward the center of a metal–metal vector. The angles shown are taken from the X-ray crystal structures.[1,3]

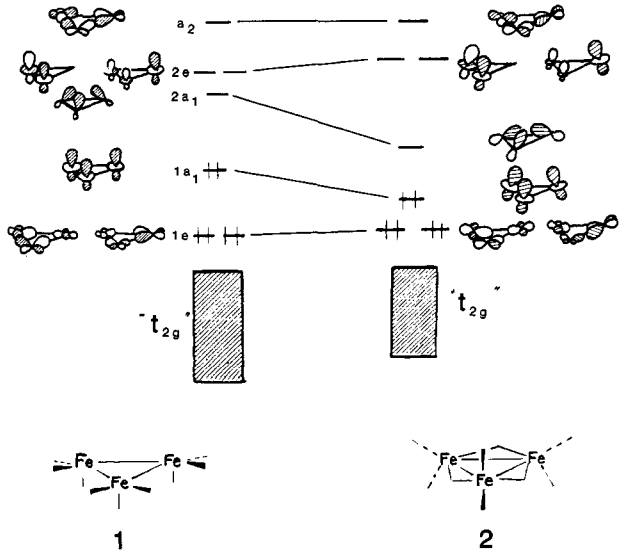

Figure 4. Effect on the frontier orbitals of an $Fe_3(CO)_9$ fragment on changing the carbonyl ligand geometry from that observed for $[Fe_3(CO)_9(CCO)]^{2-}$ and $[Os_3(CO)_9(CCO)]^{2-}$ (type 1) to that observed in $[Ru_3(CO)_9(CCO)]^{2-}$ (type 2).

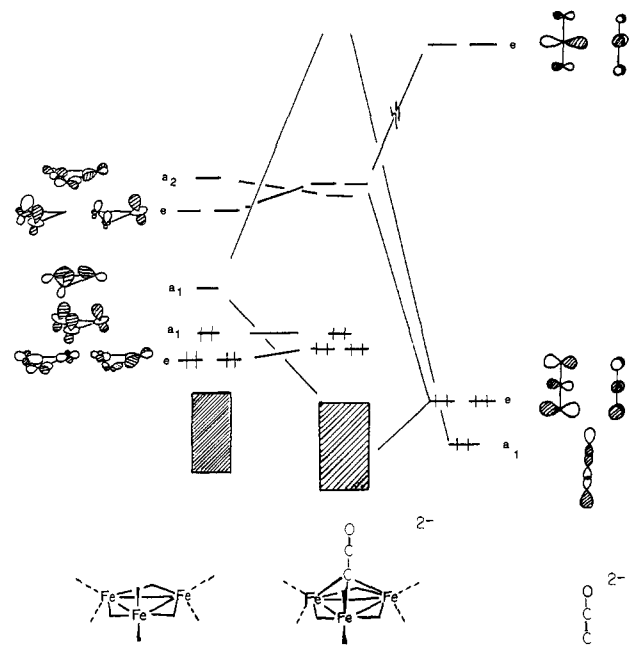

Figure 5. Interaction of the $(CCO)^{2-}$ ligand with a hypothetical $Fe_3(CO)_6(\mu\text{-}CO)_3$ fragment.

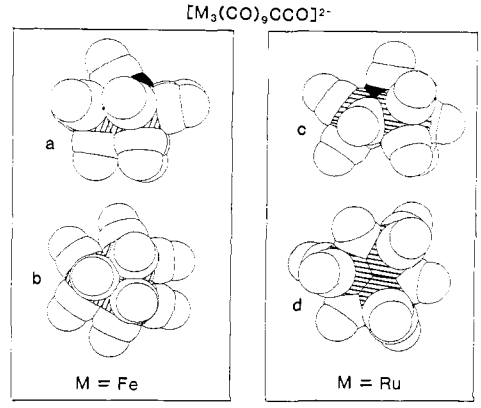

Figure 6. Space-filling models comparing the structures of $[M_3(CO)_9CCO]^{2-}$ clusters for M = Fe or Os (type 1) and M = Ru (type 2). The black atom is the α-carbon of the CCO ligand and the cross-hatched atoms are the metals. Atoms are drawn with van der Waals radii by using atomic coordinates from the X-ray crystal structures. (a) and (c) represent side views and (b) and (d) represent the view from beneath the cluster for M = Fe and Ru, respectively.

(1)–C(2)–O(2) and the perpendicular to the plane of the osmium triangle. The three Os–C(1) distances are not equal, C(1) being furthest away from the osmium atom Os(3) (toward which the CCO is tilted) by ca. 0.1 Å. Relevant bond distances and angles are listed in Table III. Positional parameters for the dianion are given in Table IV.

Structure and Bonding in the Series $[M_3(CO)_9(CCO)]^{2-}$ (M = Fe, Ru, Os). There are two basic geometries displayed by the $[M_3(CO)_9(CCO)]^{2-}$ clusters. The iron and osmium ketenylidenes belong to one class in which six equatorial and three axial carbonyls are arranged around the metal triangle and a CCO ligand caps the face of the triangle. This CCO is distinctly tilted toward one of the metal vertices (Figure 3). The structure of the ruthenium ketenylidene is different. In that case three bridging carbonyls project slightly below the metal triangle. The remaining six carbonyls are terminal. Of these, three project above the plane of the metals and three below (Figure 3). The CCO ligand again caps a triangular face of the metals, but for $[Ru_3(CO)_9(CCO)]^{2-}$ it is nearly vertical (12° tilt with respect to the vertical). It is difficult to determine whether the CCO tilt observed in the single-crystal X-ray determination is retained in solution. The low-temperature ^{13}C NMR spectrum of $[Co_3(CO)_9(CCO)]^+$

Scheme III

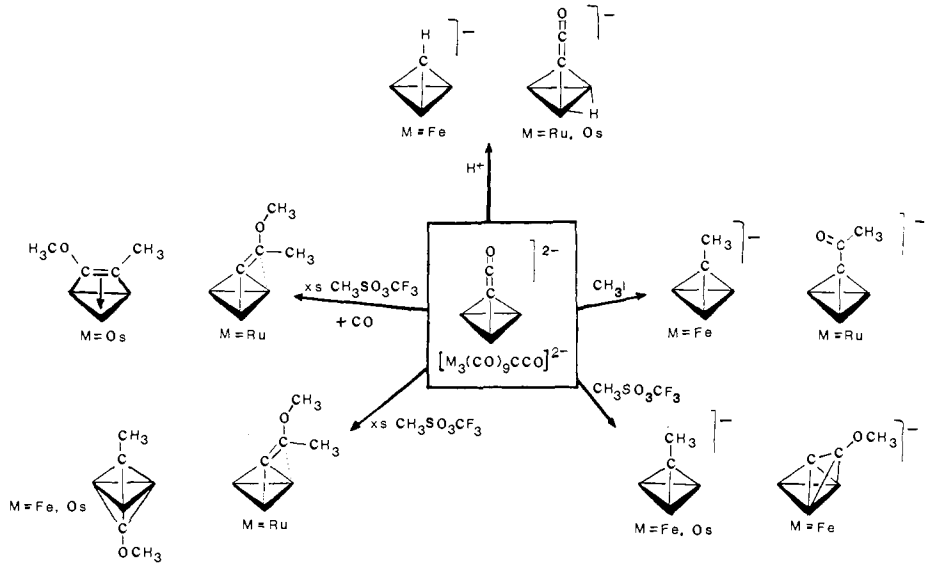

shows a set of two carbonyl resonances of relative intensity 3:6, which has been interpreted in terms of the loss of the precession motion of the CCO ligand about the cluster.[19] The low-temperature ^{13}C NMR spectrum of $[Os_3(CO)_9(CCO)]^{2-}$ is similar to that of $[Co_3(CO)_9(CCO)]^+$. Conclusive interpretation of these spectra is hampered by other possible fluxional processes, such as carbonyl turnstile rotations and intermetal carbonyl exchange (merry-go-round) which can occur in the same energy regime.[19,21] A molecular orbital description of the bonding in $[Ru_3(CO)_9(CCO)]^{2-}$ (type 2 structure) has been discussed in an accompanying paper, and some MO descriptions of the type 1 ketenylidenes have appeared in the literature.[19,20] In the present research, the difference in bonding between the two classes of ketenylidenes (types 1 and 2 in Figure 3) was explored by extended Hückel calculations. Figure 4 shows the frontier orbitals for $Fe_3(CO)_9$ fragments having these two types of CO orientations. The energetically preferred orientation of the CCO ligand over a triiron framework is one in which the CCO ligand is tilted toward a metal vertex, but the potential energy surface for tilting the CCO ligand is very shallow. the tilted CCO is favored over the perpendicular disposition by 0.2 eV (3 kcal/mol). The energy difference between CCO tilting toward a metal or toward the center of a metal–metal bond is negligible.

The effect of changing to the carbonyl geometry of the ruthenium ketenylidene (type 2) is to direct the frontier orbitals of the fragment more strongly toward the position of the α-carbon. The interaction of the modified $Fe_3(CO)_9$ fragment (type 2 of Figure 3) and the $(CCO)^{2-}$ moiety is shown in Figure 5 and is similar in nature to that previously derived for $[Co_3(CO)_9(CCO)]^+$ (type 1).[19] However, in the type 2 geometry tilting the CCO ligand over either a ruthenium center or a ruthenium–ruthenium bond destabilized the cluster by 2 kcal/mol. The effect of this tilt is to weaken the interaction of the a_1 CCO molecular orbital with the frontier orbitals of the metal base without a compensating increase in interaction of the e orbitals. Thus the extended Hückel calculations agree with the CCO dispositions observed by X-ray diffraction, but the calculated energy differences between the various conformations are too small to be reliable. Of greater significance are the nature of the HOMO and the steric differences between the type 1 and 2 structures. Space-filling drawings calculated from the crystallographic coordinates of $[Ru_3(CO)_9(CCO)]^{2-}$ and $[Fe_3(CO)_9(CCO)]^{2-}$ are shown in Figure 6.[1,3] The model of $[Os_3(CO)_9(CCO)]^{2-}$ is essentially the same as for its triiron homologue. The two key points that these models illustrate are that the tilted CCO disposition in concert with the axial arrangement of the carbonyls in the Fe_3 and Os_3 clusters results in a much greater degree of exposure of the α-carbon (black in the diagrams) than for the Ru_3 cluster and that the metals are more highly exposed in the Ru_3 cluster than in either the Fe_3 or Os_3 ketenylidenes. Additionally, the exposed metal region shown for the Ru_3 cluster (molecule d of Figure 6) corresponds to the site of highest electron density for the HOMO of the Ru_3 ketenylidene.[4]

Comparison of $[M_3(CO)_9(CCO)]^{2-}$ Reactivities. In general the dianionic series of ketenylidenes $[M_3(CO)_9(CCO)]^{2-}$ (M = Fe, Ru, Os) behave as nucleophiles. Although they are from the same group in the periodic table, the identity of the metals has a profound influence on the reactions of the CCO ligand. The rich pattern of reactivity observed for the triad of anionic ketenylidene compounds is summarized in Scheme III. The products that can be derived from the CCO ligand include methylidyne, alkylidyne, vinylidene, and acetylide species. Facile C–C bond formation and cleavage via transfer of ligands between the α-C and metals is characteristic of these three-metal clusters. This C–C bond cleavage appears to be facilitated by conformations in which the CCO ligand is tilted toward a metal atom of the cluster.

Acknowledgment. The assistance of Stanton Ching and Don J. Wang with the crystallographic solution is gratefully acknowledged. M.J.W. acknowledges a NATO/SERC postdoctoral fellowship. P.L.B. acknowledges an NSF predoctoral fellowship. This research was supported by the NSF Synthetic Inorganic Organometallic Program.

Supplementary Material Available: atom numbering scheme and tables of anisotropic thermal parameters, bond angles and distances, and positional parameters for all atoms of **1** (19 pages); a table of F_o and F_c for **1** (110 pages). Ordering information is given on any current masthead page.

(19) D'Agostino, M. F.; Mleekuz, M.; Kolis, J. W.; Sayer, B. G.; Rodger, C. A.; Halet, J.-F.; Saillard, J.-Y.; McGlinchey, M. J. *Organometallics* **1986**, *5*, 2345.
(20) Barreto, R. D.; Fehlner, T. P.; Hsu, L.-Y.; Jan, D.-Y.; Shore, S. G. *Inorg. Chem.* **1986**, *25*, 3572.
(21) Band, E.; Muetterties, E. L.; *Chem. Rev.* **1978**, *78*, 639, and references contained therein.
(22) (a) Schilling, B. E. R.; Hoffmann, R. *J. Am. Chem. Soc.* **1979**, *101*, 3456. (b) Chesky, P. T.; Hall, M. B. *Inorg. Chem.* **1981**, *20*, 4419.
(23) Bogdan, P. L.; Sabat, M.; Sunshine, S. A.; Woodcock, C.; Shriver, D. F., manuscript in preparation.